第 34 卷第 12 期　　焊　接　学　报　　Vol. 34　No. 12
2013 年 12 月　　TRANSACTIONS OF THE CHINA WELDING INSTITUTION　　December　2013

# 镁合金表面搅拌摩擦原位复合材料化的新方法

黄永宪[1]，　王天昊[1]，　吕世雄[1]，　刘会杰[1]，　敖　峰[2]
（1. 哈尔滨工业大学 先进焊接与连接国家重点实验室，哈尔滨　150001；
2. 扬州秋源压力容器制造有限公司，扬州　225115）

**摘　要：** 为了解决搅拌摩擦加工在进行复合材料制备过程中增强相需预置，及在基体中分布不均的问题，提出表面搅拌摩擦原位复合材料化的新方法. 利用搅拌头在轧制态 AZ31 镁合金板材上进行表面复合材料制备，并对制备的复合材料进行显微观察、微观硬度测试、表面耐磨度测试. 结果表明，相较于预置搅拌摩擦加工制备复合材料的方法，文中方法能够使增强相在基体中分布更加弥散、均匀，从而进一步提高复合材料层的显微硬度，以及材料表面的耐磨度，同时简化了搅拌摩擦加工制备复合材料的工艺过程.

**关键词：** 镁合金；搅拌摩擦加工；原位；表面复合材料化
**中图分类号：** TG456　　**文献标识码：** A　　**文章编号：** 0253－360X(2013)12－0025－04

黄永宪

## 0　序　　言

镁合金由于质量轻，作为结构材料在航空航天领域被广泛使用. 然而其力学性能较低，例如硬度以及耐磨度较低，限制了其进一步应用[1,2]. 为了解决该问题，一般可以采用在镁合金基体上制备复合材料的方法. 2003 年 Mishra 等人[3]提出了利用搅拌摩擦加工进行表面复合材料制备的方法. 近年来，人们对搅拌摩擦加工(friction stir processing，FSP)制备金属基复合材料的方法进行了大量研究工作. 重点在于如何使增强相均匀、弥散地分布在金属基体中. 在以往利用 FSP 制备复合材料时，需将增强相预置于金属基体表面，再进行 FSP[4－10]. 利用上述方法进行复合材料制备时，容易发生增强相颗粒的滑移，进而使得其在基体中分布不均.

文中提出搅拌摩擦原位制备表面复合材料新方法，利用中空搅拌头在材料表面直接进行 FSP，增强相沿搅拌头的中空送料通道进入搅拌头与被加工材料的作用界面，颗粒被轴肩直接搅压入基体中，未发生颗粒的飞溅及推移，保证增强相在基体中的均匀性. 试验结果表明，使用该方法进行表面复合材料的制备可提高增强相在基体中的均匀性，提高复合层的显微硬度以及材料表面的耐磨度.

**收稿日期：** 2012－09－21
**基金项目：** 国家自然科学基金资助项目(50904020)；中央高校基础科研业务费专项资金资助项目(HIT. NSRIF. 2012007)

## 1　试验过程

试验中所使用的材料为轧制态的 AZ31(Mg－3.12% Al－1.12% Zn－0.42% Mn)镁合金板材，厚度为 4 mm，增强相颗粒为平均直径为 10 μm 的 SiC 颗粒(纯度为 99.9%).

与传统搅拌头不同，文中采用无针中空搅拌头. 搅拌头形貌如图 1 所示. 具体尺寸为轴肩直径 24 mm，中空孔径 8 mm，轴肩凹形端面与平面的夹角为 1°. 图 1a 所示为搅拌头整体；图 1b 所示为搅拌头的出料口，增强相颗粒由此孔流出，从而进入轴肩与母材之间的界面；图 1c 所示为搅拌头的送料孔，增强相颗粒由此进入搅拌头的中空孔道.

试验所采用的焊接设备为 FSW－3LM－003 型龙门式数控搅拌摩擦焊机. 最大功率 15 kW，最高旋转频率 3 000 r/min，运动精度 ±0.25 mm. 选定搅拌头旋转频率为 400 r/min；焊接速度为 30 mm/min；搅拌头倾角为 1°；压入量 0.3 mm. 焊后采用 Olympus－MPG3 光学显微镜对复合层及金属基体进行显微分析，同时对增强相颗粒与基体的界面进行显微分析.

采用 HVS－1000Z 显微硬度测试机进行显微硬度测试，加载载荷为 0.49 N；采用 HT－1000 型高温摩擦磨损试验机进行材料表面耐磨度分析，试验所使用的氮化硅陶瓷球直径为 8 mm，磨损载荷 4.9 N，陶瓷磨损球旋转频率为 300 r/min，磨损时间为 6 min.

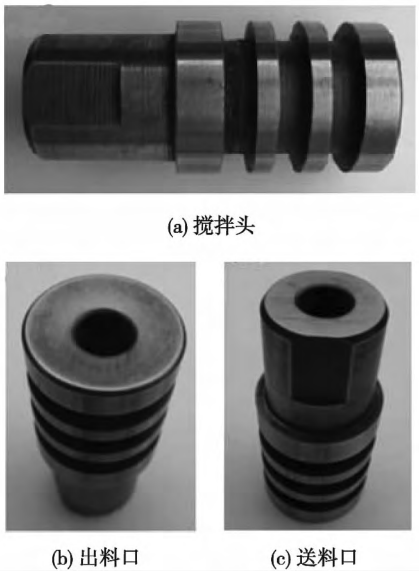


**图 1 搅拌摩擦原位复合材料化搅拌头**

Fig. 1 View of tool for In-situ fabrication of surface composite by FSP

## 2 技术原理

搅拌摩擦原位复合材料化过程如图 2 所示. 过程中增强相沿搅拌头中的中空送料通道进入搅拌头与被加工材料的作用界面,最后被搅拌头轴肩的凹形端面搅压入材料基体中,从而实现表面复合材料的制备.

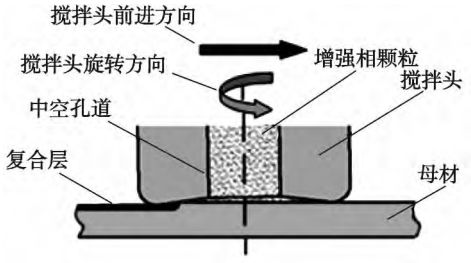


**图 2 搅拌摩擦原位复合材料化过程示意图**

Fig. 2 Schematic illustrations of In-situ fabrication of surface composite by FSP

相较于以往预置增强相的 FSP 表面复合材料制备,该过程中不会发生颗粒飞溅以及推移,进而保证了增强相在基体中分布的均匀性. 此外该方法不用在材料表面进行预加工,简化了工艺过程.

## 3 试验结果

经过搅拌摩擦原位复合材料化后,母材表面制备出一层复合层,其表面形貌显微图像如图 3 所示,通过 FSP 制备表面复合材料后,材料表面存在 SiC 颗粒.

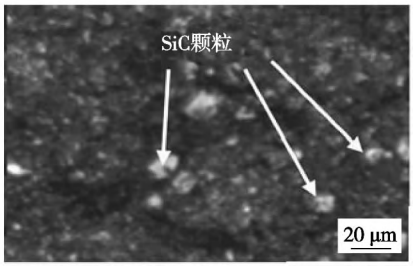


**图 3 复合材料表面光学显微组织形貌**

Fig. 3 Optical micrograph of surface of composite material

### 3.1 微观结构

图 4 显示为对加工后试样的横截面进行显微观察. 图 4a 为直接 FSP 后的试样横截面显微图像,其由搅拌区(stir zone, SZ)、热力影响区(thermal-mechanical affected zone, TMAZ)、以及基体(base metal, BM) 3 部分组成,观察可知,搅拌区内的晶粒十分细小,热力影响区以及基体内的晶粒尺寸较大;图 4b 为原位复合材料化后的试样横截面显微图像,其也由上述的搅拌区、热力影响区以及基体 3 部分组成,但在复合材料化后试样的搅拌区内,均匀、弥散地分布着 SiC 颗粒,通过观察图 4b 可知,在上述工艺参数下所制备的材料表面的复合层厚度约为

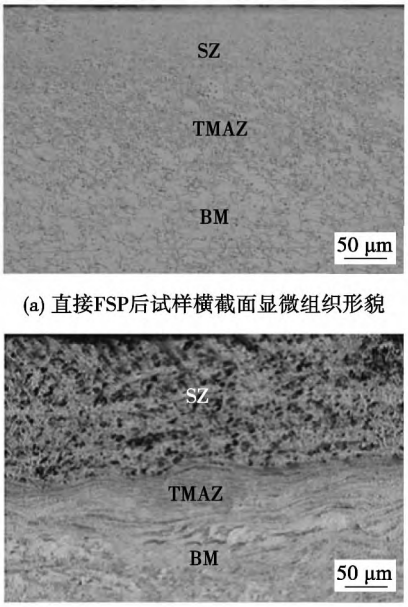


**图 4 试样横截面光学显微组织形貌**

Fig. 4 Optical micrograph of cross section of specimen

250 μm，且增强相在基体中并未发生团聚，而是均匀弥散地分布在其中.

对直接 FSP 后、原位复合材料化后的搅拌区以及基体进行放大，如图 5a 显示的是直接 FSP 后搅拌区显微图像，晶粒平均尺寸达到了 5.4 μm；图 5b 显示的是原位复合材料化后搅拌区显微图像，其中 SiC 颗粒平均直径为 10 μm，且不发生团聚，晶粒平均尺寸为 1.4 μm；图 5c 显示的是母材区域的显微图像，晶粒平均尺寸为 28.3 μm.

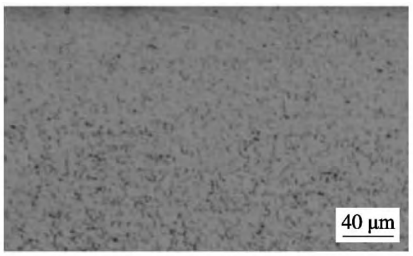


(a) 直接FSP后搅拌区

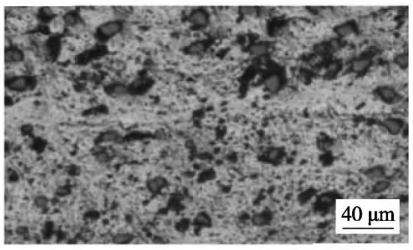


(b) 原位复合材料化后搅拌区

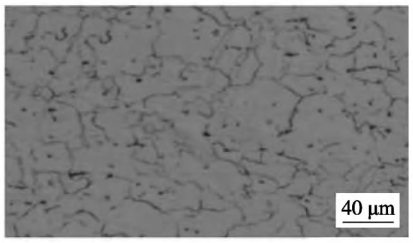


(c) 母材区

**图 5　各区域进一步放大的光学显微组织形貌**

Fig. 5　Magnified optical micrograph of related areas

### 3.2　显微硬度

图 6 表示的是图 4a，b，及未加工材料基体由表面至基体的硬度值分布. 材料基体平均硬度值为 625.5 MPa；而经过 FSP 后，搅拌区晶粒细化，其平均硬度值达到 845.1 MPa；原位复合后，搅拌区内的晶粒更加细小，这是由于在进行表面原位复合材料化过程中，第二相和增强相颗粒同时钉扎晶粒，限制其长大，晶粒细化程度进一步提升，硬度也进一步升高，因此搅拌区平均硬度值达到 1 366.7 MPa，此外由于增强相颗粒自身平均硬度值为 1 985.3 MPa，很大程度上提高了复合层硬度值.

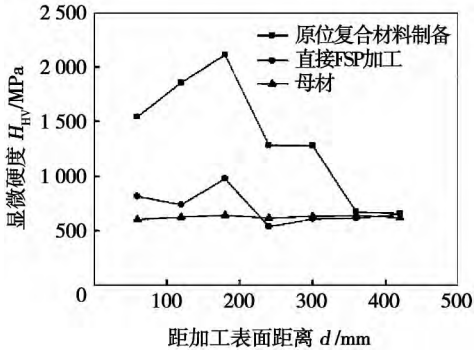


**图 6　横截面显微硬度分布**

Fig. 6　Microhardness profile of cross-section of specimen

### 3.3　摩擦磨损试验

对母材表面以及经过表面原位复合材料化后的材料表面进行表面摩擦磨损试验. 磨损后磨痕的显微图像分别如图 7a，b 所示，对比图 7a 与 7b 可以发现，经过原位复合材料化后，材料表面形成一层复合层，其能够有效降低磨损作用，使表面磨痕变窄.

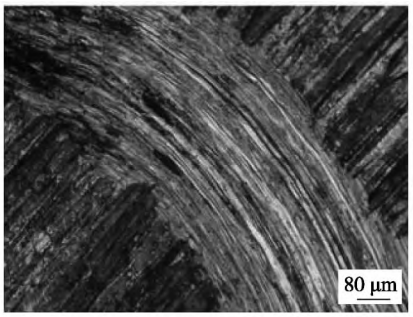


(a) 母材表面磨痕

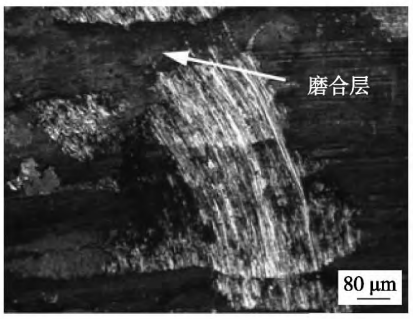


(b) 经过表面复合后的材料表面磨痕

**图 7　摩擦磨损试验后材料表面磨痕光学显微组织形貌**

Fig. 7　Optical micrographs of worn surfaces of specimen

对摩擦磨损试验中使用的陶瓷球上的磨痕进行显微分析，对母材表面进行摩擦磨损试验所使用的陶瓷球的磨痕直径约为 800 μm，根据球径为 8 mm，得出陶瓷球消耗高度约为 20.0 μm；对复合后材料表面进行摩擦磨损试验所使用的陶瓷球磨痕直径约

为 1 000 μm，得出陶瓷球消耗高度为 31.4 μm. 因此使用于母材表面陶瓷球上的磨痕尺寸要明显小于使用于在表面复合后材料表面的陶瓷球上的磨痕尺寸，进一步证明了课题所制备的复合层使材料表面耐磨性有了很大的提高.

## 4 结 论

(1) 提出了搅拌摩擦原位复合材料化的新方法，很好解决了增强相颗粒容易在母材表面发生推移及飞溅的问题，进而保证了增强相颗粒在材料基体中分布的均匀性与弥散性. 同时在加工参数为旋转频率 400 r/min，焊接速度 30 mm/min，搅拌头倾角 1°，压入量 0.3 mm 时，复合效果最优，能形成厚度为 250 μm，增强相颗粒分布均匀弥散的复合层，且其与基体的连接较好.

(2) 经 FSP 后晶粒发生回复再结晶，晶粒长大过程中被析出的第二相钉扎，限制其长大，进而发生晶粒细化；在进行表面复合材料化 FSP 后，晶粒发生回复再结晶，但在长大过程中钉扎晶粒限制其长大的不仅有 $\beta$ 相，还有增强相颗粒，因此晶粒细化程度进一步提高.

(3) 经过表面原位复合材料化后，材料复合层的显微硬度以及材料表面的耐磨性均有显著的提高，其强化方式为细晶强化以及增强相自身高硬度、高耐磨度强化. 复合层的显微硬度由母材的 625.5 MPa 增加至 1 366.7 MPa，增强相颗粒自身的显微硬度为 1 985.3 MPa. 材料表面对磨损试验中陶瓷球的消耗高度由母材消耗的 20.0 μm 升高至 31.4 μm.

## 参考文献:


[1] 张 华，林三宝，吴 林，等. AZ31 镁合金搅拌摩擦焊接接头力学性能 [J]. 焊接学报，2003，24(5)：65 - 69.
Zhang Hua，Lin Sanbao，Wu Lin，*et al*. Current progress and prospect of friction stir welding [J]. Transactions of the China Welding Institution，2003，24(5)：65 - 69.

[2] 杨素媛，张保垒. 厚板 AZ31 镁合金搅拌摩擦焊焊接接头的组织与性能 [J]. 焊接学报，2009，30(5)：1 - 5.
Yang Suyuan，Zhang Baolei. Microstructures and mechanical properties of thick AZ31mag-nesium alloy welded joint by friction stir welding [J]. Transactions of the China Welding Institution，2009，30(5)：1 - 5.

[3] Mishra R S，Ma Z Y，Charit I，*et al*. Friction stir processing：a novel technique for fabrication of surface composite [J]. Material Science and Engineering A，2003，341：307 - 310.

[4] Morisada Y，Fujii H，Nagaoka T，*et al*. Effect of friction stir processing with SiC particles on microstructure and hardness of AZ31 [J]. Material Science and Engineering A，2006，433：50 - 54.

[5] Lee Wonbae，Lee Changyong，Kim Myoungkyun，*et al*. Microstructures and wear property of friction stir welded AZ91 Mg/SiC particle reinforced composite [J]. Composites Science and Technology，2006，66：1513 - 1520.

[6] Mishra R S，Ma Z Y. Friction stir welding and processing [J]. Materials Science and Engineering R，2005，50：1 - 78.

[7] Lee C J，Huang J C，Hsieh P J. Mg based nano-composite fabricated by friction stir processing [J]. Scripta Materialia，2006，54：1415 - 1420.

[8] 马宗义. 一种表面搅拌摩擦加工方法以及专用加工工具：中国，10135148.1 [P]. 2008 - 07 - 02.

[9] 马宗义. 一种表面/块体金属基复合材料及其制备方法：中国，10248824.X [P]. 2009 - 12 - 28.

[10] 钱锦文，李京龙，熊江涛，等. 搅拌摩擦加工原位反应制备 Al3Ti-Al 表面复合层 [J]. 焊接学报，2010，31(8)：61 - 64.
Qian Jinwen，Li Jinglong，Xiong Jiangtao，*et al*. In-situ synthesized Al3Ti-Al surface composites by friction stir processing [J]. Transactions of the China Welding Institution，2010，31(8)：61 - 64.

[11] Chang C I，Lee C J，Huang J C. Relationship between grain size and Zener-Holloman parameter during friction stir processing in AZ31 Mg alloys [J]. Scripta Materialia，2004，51：509 - 514.


**作者简介：** 黄永宪，男，1979 年出生，博士，副教授. 主要从事搅拌摩擦焊技术方面的科研和教学工作. 发表论文 30 余篇，授权专利 20 余项. Email：yxhuang@ hit. edu. cn

Wensheng, CAI Qingshan (State Key Laboratory for Powder Metallurgy, Central South University, Changsha 410083, China). pp 17 – 20

**Abstract:** The interface characteristics between W and ferrite steel (FS) diffusion welded with a V interlayer of 0.5mm in thickness was investigated in vacuum hot pressing furnace at 1 050 ℃ for 1h and 10 MPa. Microstructures, element compositions and micro-hardness of joint were analyzed and tested with field-emission scanning electron microscopy (FE-SEM), energy dispersive spectroscopy (EDS) and nanoindenter, respectively. Tensile strength was tested with mechanical test machine. Results showed that, a reliable bonding on W/FS interfaces by means of diffusion welding between matrix and V interlayer was obtained. The W/FS joint is a multilayer sandwich structure, which includes the transition zone of W/V, the residual V interlayer and the diffusion layer of V/FS. Meanwhile, the transition zone of W/V was mainly composed of a solid solution structure and the V/FS diffusion layer with the highest hardness where there was a definite structure of V/VC layer/decarburized layer/FS. The tensile strength of joint reaches 75MPa and V/FS interface is main fracture source because of containing brittle VC phase.

**Key words:** tungsten; steel; diffusion bonding; interlayer; microstructure

**Elimination of lazy S defect in friction stir welded joint of 20mm-6063 alumimum alloy** HE Diqiu, YE Shaoyong, WANG Jian (State Key Laboratory of Complicated Equipment Design and Extreme Manufacturing, Central South University, Changsha 410083, China). pp 21 – 24

**Abstract:** 20 mm thick 6063 aluminum alloy plate were joined by friction stir welding with gas protection. The result showed that the sound joint without lazy S can be achieved. The average tensile strength of welds is 148.9 MPa, which is 81.9% of that of the base metal. Optical microscopy revealed the stir zone presents particularly fined equiaxed gains formed by dynamic recrystallization. The microstructure in TMAZ, in which some degree of dynamic recrystallization occurs, consists of deformed gains. The result shows that lazy S of 6063 aluminum alloy can be eliminated by FSW with gas protection.

**Key words:** friction stir welding; 6063 aluminum alloy; lazy S; microstructure

**A novel method of in-situ fabrication of Mg surface composites by friction stir process** HUANG Yongxian[1], WANG Tianhao[1], LÜ Shixiong[1], LIU Huijie[1], AO Feng[2] (1. State Key Laboratory of Advanced Welding and Joining, Harbin Institute of Technology, Harbin 150001, China; 2. Yangzhou Qiuyuan Pressure Vessel Manufacturing Co., Ltd., Yangzhou 225115, China). pp 25 – 28

**Abstract:** In the previous fabrication process of surface composite by friction stir process (FSP), the reinforcement phases were needed to preplace on the base metal. However, these particles didn't distribute very well in the stir zone. Therefore, friction stir process without preplacing reinforcement phase was proposed to prepare the surface composite. A FSP tool consisting of only shoulder was designed, and used to fabricate the surface composite on the AZ31 plate as-rolled. Microstructure was analyzed by optical microscope and SEM. The microhardness and surface wear resistance tests of specimens show that the particle reinforcement are more homogeneous, so that the microhardness and wear resistance increase, and at the same time, the preparation work is simplified to a great extent.

**Key words:** magnesium alloy; friction stir process; in-situ; surface composites

**Characteristics of bypass-current MIG-TIG double-sided welding of stainless steel** MIAO Yugang[1], HAN Duanfeng[1], WU Bintao[2], XU Xiangfang[2], LI Xiaoxu[2] (1. National Key Laboratory of Science and Technology on Underwater Vehicle, Harbin Engineering University, Harbin 150001, China; 2. College of Shipbuilding Engineering, Harbin Engineering University, Harbin 150001, China). pp 29 – 32

**Abstract:** By using 6mm thick 304 stainless steel plate as base metal, the bypass-current double-sided arc welding experiments were carried out. The results showed the technology can obtain the stable process and good weld appearance. The other remarkable advantages such as increasing joint penetration, deceasing welding defects, enhancing production efficiency, reducing welding cost were also achieved. The reliable joining of 6mm thick 304 stainless steel was realized at welding current of 110 A. Furthermore, the melting efficiency of bypass-current double-sided arc welding can reach 60.2%, more than 17.6% of TIG welding and 43.2% of bypass-current MIG welding. The tensile results showed the strength of the joints can reach 776.5MPa, about 95% of that of base metal. The fracture occurs at the heat-effect zone, and the angle between fracture line and stress direction is 45°. The fracture appearance is gray, which shows the characteristics of ductile fracture.

**Key words:** bypass-current MIG-TIG double-sided welding; melting efficiency; tensile strength; weld appearance

**Test and analysis of arc pressure measurement in coupling arc electrode TIG welding** HUANG Yong[1,2], HAO Yanzhao[2], QU Huaiyu[2], LIU Ruilin[2] (1. State Key Laboratory of Gansu Advanced Non-ferrous Metal Materials, Lanzhou University of Technology, Lanzhou 730050, China; 2. Key Laboratory of Non-ferrous Metal Alloys and Processing, The Ministry of Education, Lanzhou University of Technology, Lanzhou 730050, China). pp 33 – 36

**Abstract:** A kind of coupling arc tungsten electrode was developed to decrease arc pressure remarkably, avoid undercut and humping weld. Adopting this method, high-quality TIG welding with relative higher speed can be achieved. The TIG arc pressure of this kind of welding process was tested to investigate the influence of the parameters on distribution of arc pressure. Compared with the traditional TIG arc, the TIG arc pressure with coupling arc electrode is much lower with the same parameters, and decreases with the increase of arc length, the increase of electrode extended length, the decrease of current, the increase of the electrode gap width and the increase of the electrode diameters. The arrangement of the influence in decreasing order is current, electrode extended length, arc length and electrode diameter, electrode gap width.